Revisiting the thermal behavior of dipyrone

R. S. Medeiros[1] · A. P. G. Ferreira[1] · E. T. G. Cavalheiro[1]

Abstract

Although some thermoanalytical studies regarding thermal analysis of dipyrone sodium monohydrate had already been presented in literature, results are incomplete once no evolved gas analysis has been presented. In addition, the inorganic residue should also be better characterized regarding the presence of sodium sulfate or sodium hydrogen sulfite, once the amount of residue varies depending on experimental conditions. In this work, the thermal degradation of dipyrone sodium monohydrate was revisited regarding evolved gases, intermediates produced during heating and inorganic residue. Thus, dipyrone sodium monohydrate was analyzed using TG/DTG/DTA, DSC, hot-stage microscopy, TG–FTIR and HPLC–MS looking for proposing a thermal behavior mechanism for this important pharmaceutical. Moreover, inorganic residue was investigated by XRD and FTIR. The evolved gases were detected and identified in the following sequence: water, sulfur dioxide, methylamine, isocyanic acid, benzene, ammonia and carbon dioxide. Regarding the inorganic fraction, intermediates were collected at 500 and 1000 °C and characterized as Na_2SO_4 in dry air atmosphere. From these data obtained by combining results from thermoanalytical techniques with those from HPLC–MS, FTIR and XRD, a mechanism for the thermal behavior of dipyrone sodium monohydrate was proposed.

Keywords Dipyrone · Metamizole · Anti-inflammatory · Evolved gas analysis · Thermal behavior mechanism

Introduction

Dipyrone as its monohydrate sodium salt [sodium *N*-(2,3-dimethyl-5-oxo-1-phenyl-3-pyrazolin-4-yl)-*N*-methylaminomethanesulfonate (Fig. 1)] also called metamizole is one of the most popular analgesic and antipyretic drug worldwide.

It is considered a nonsteroidal anti-inflammatory drug, presenting analgesic, antipyretic and weak anti-inflammatory action [1]. Although its mechanism of action is still not fully elucidated, some authors proposed its action through the inhibition of cyclooxygenase enzymes [1], that are responsible for catalyzing the production of prostaglandins, the lipids responsible for inducing the inflammation, that also present antinociceptive effect.

Dipyrone was marketed freely from 1922 to 1970s in some countries, when it was verified possible risk to health, once it can cause agranulocytosis [1, 2]. This is a condition in which decreasing of white blood cell in body occurs [1]. Other countries maintained the commercialization, making metamizole one of the mostly marketed non-opioid analgesics used for treatment of pain and fever in the world [3].

When thermal analysis is combined with spectroscopic techniques, it allows the complete study of the thermal behavior of drugs and many compounds, including thermal stability, thermal decomposition pathways, characterization of intermediates, physical transformations, purity evaluation, determination of melting and crystallization points, study of polymorphic transitions, evolved gas analysis, among others [4–7].

In the literature, there is a study from Ribeiro et al. [7] concerning thermal analysis of dipyrone and other analgesic drugs, involving the investigation of their thermal stability and thermal decomposition by TG/DTG and DSC. However, the gases evolved during decomposition of the samples were not fully described.

In other work, the authors characterized the thermal behavior of dipyrone and other pharmaceutical actives using TG/DTG and DSC. In this case, thermogravimetry was performed up to 480 °C. DSC curves evidenced the

✉ E. T. G. Cavalheiro
cavalheiro@iqsc.usp.br

1   Instituto de Química de São Carlos, Universidade de São Paulo, Av. Trabalhador São-carlense, 400, São Carlos, SP 13566-590, Brazil
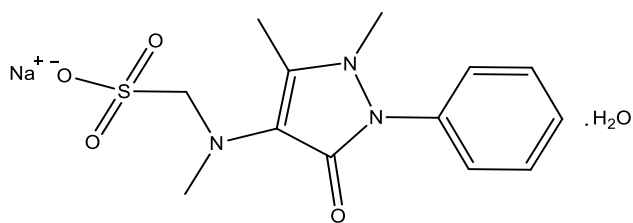
Fig. 1 Structural formula of sodium dipyrone monohydrate

characteristic peaks of water loss, melting and decomposition of the drug [8].

Isaacs et al. investigated the possibility of determining adulteration of illicit drugs with dipyrone. In their studies, they found that the drug thermally decomposed during analysis by GC or GC–MS resulting in aminopyrine and 4-methylaminoantipyrine. In HPLC or HPLC–MS, a hydrolytic process generates solely 4-methylaminopyrine. This hydrolytic event also produced sodium hydrogen sulfite ($NaHSO_3$) [9].

From these studies, a doubt rises up regarding the actual nature of the inorganic residue once Ribeiro et al. [7] claim that the residual inorganic material is Na_2SO_4 based on a qualitative test, while Isaacs et al. found that $NaHSO_3$ can be formed during a hydrolytic process [9].

Therefore, the literature lacks in the detailed description of gases evolved during dipyrone sodium monohydrate heating as well as the nature of inorganic residue must be better investigated which motivated revisiting this subject. Thus, in the present work, a detailed investigation of dipyrone sodium monohydrate thermal degradation using TG/DTG, DTA, DSC, hot-stage microscopy, TG–FTIR, XRD, FTIR and HPLC–MS is presented. Furthermore, the characterization of intermediate and final inorganic residue was performed. All these data combined allowed a proposition of a complete thermal behavior mechanism for this important pharmaceutical.

Experimental

Dipyrone sodium monohydrate (DIP, 98.0%) was purchased from Sigma-Aldrich (USA) and used as received.

Thermal analysis

TG/DTG/DTA curves were obtained using a simultaneous TG/DTA SDT-Q600 module managed by the Thermal Advantage® for Q-Series software (v.5.5.24) both from TA Instruments. The measurements were taken in dynamic dry air and nitrogen atmospheres, flowing at 50 mL min^{-1}, using sample mass of 7.0 ± 0.2 mg, temperature range of 25–1000 ºC, heating rate

of 10 °C min^{-1} in open α-alumina sample holders. Different conditions as sample mass (3.0–17 mg); sample presentation (powder or pellets) and heating rate (10–25 °C min^{-1}) were also used to investigate the nature of the inorganic residue at 1000 °C, as described in the text.

DSC curves were obtained in a Q10 Differential Scanning Calorimetric module, controlled by Thermal Advantage® for Q-Series software (v.5.5.24), both from TA Instruments, using sample mass of 5.0 ± 0.1 mg, at a heating rate of 10 °C min^{-1}, under dynamic N_2 atmosphere, flowing at 50 mL min^{-1}, in closed aluminum sample holders with a pin hole ($\varnothing = 0.7$ mm) in the center of the lid, in the heating mode, between 25 and 275 °C.

Evolved gas analysis

An SDT-Q600 (TA Instruments) module coupled to an iS10 FTIR (Nicolet) spectrophotometer was used to characterize the gaseous products evolved during the heating of dipyrone sodium monohydrate. The transfer line was composed of a thermally insulated 120 cm long stainless-steel tube with 2 mm internal diameter, heated at a constant temperature of 230 °C. The FTIR spectra were recorded in a Nicolet iS10 spectrophotometer with a DTGS detector in a gas cell heated at constant temperature of 250 °C. The interferometer and the compartment of the gas cell were purged with nitrogen. The thermogravimetric curve was obtained in dynamic N_2 atmosphere flowing at 60 mL min^{-1}, heating rate of 10 °C min^{-1} and sample mass of *c.a.* 15 mg.

Hot-stage microscopy

Hot-stage microscopy was performed using a Mettler-HS82 apparatus coupled to an Olympus BX51 optical microscope equipped with a SC30 Olympus digital camera. Dipyrone sodium monohydrate thermal behavior was investigated in the range of 200–230 °C using a heating rate of 4 °C min^{-1}.

Elemental analysis

Elemental analysis was performed in a Flash Smart system (Thermo Scientific), using 10.0 mg of dipyrone sodium monohydrate.

X-ray diffraction

X-ray diffractograms were obtained in an Ultima IV (Rigaku) diffractometer, equipped with a copper tube radiation source in normal scan mode. Data were acquired in the mode 2θ/θ with scan from 5° to 60°, with one step of 0.02° s^{-1} rate of 0.5° min^{-1}.

Infrared spectroscopy

The vibrational spectra in the infrared region were obtained in an IRAffinity-1 FTIR spectrometer (Shimadzu) between 4000 and 400 cm^{-1}, resolution of 4 cm^{-1} and 64 scans. The samples were prepared as KBr pellets in the proportion of 5.0 mg of sample to 95 mg of KBr.

High-performance liquid chromatography coupled to mass spectrometry (HPLC–MS)

The intermediate of decomposition at 235 °C was characterized by HPLC–MS. The sample was heated up to 235 °C in the thermobalance, under the same conditions used in TG experiments mentioned above. The resulting solid sample was collected, solubilized in water and injected in the HPLC (Accela High Speed LC—Thermo Scientific) coupled to a mass spectrometer MS (Thermo Scientific). A C18—2.0 μm, 15 cm, Shimadzu VP-ODS—column was used [10].

The mobile phase used was a mixture of water (20%) and methanol (80%) (*v/v*), flowing at 1 mL min^{-1} [10]. Mass analysis was performed with MS system with an electrospray (ISE) source, in the positive mode. Data were obtained in the range of 50–500 m/*z* in the total ion chromatogram (TIC).

Results and discussion

Elemental analysis (C, H, N) results for the sample used in this work are presented in Table 1.

These results revealed good agreement between experimental data and calculated values for dipyrone sodium monohydrate, according to the structural formula represented in Fig. 1, suggesting high purity degree of the sample.

Figure 2 depicts TG/DTG and DTA curves of dipyrone sodium monohydrate in dynamic atmospheres of dry air and N_2. Table 2 presents quantitative data regarding the events observed in these curves in both atmospheres, including mass loses, temperature ranges and peak temperatures.

Under air, TG curve (Fig. 2a) revealed an initial dehydration process in the 53.9–119.1 °C range. The decomposition

Table 1 Results for C, H and N elemental composition of dipyrone sodium monohydrate

Sample[a]	Element, exp(calc)/%		
	C	H	N
Dipyrone sodium monohydrate	44.5 (44.4)	4.97 (5.16)	11.9 (11.9)

[a] mol mass 351.35 g mol^{-1}

takes place in two steps, one from 230.8 to 270.4 °C and other one from 270.4 to 651.6.0 °C. These mass losses are followed by a fourth mass loss of 8.9% that corresponds to the burn of carbonaceous materials, with a final residue of 19.5%.

The DTA curve (Fig. 2b) in air showed one broad endothermic peak at 105.1 °C assigned to dehydration of dipyrone sodium monohydrate and a sharp endothermic melting peak at 235.0 °C, followed by a sharp exothermic peak at 245.4 °C attributed to the decomposition of the drug. Above 600.0 °C, an exothermic process takes place centered at 701.5 °C due to the burn of carbonaceous material and a low-intensity endothermic peak is present at 855.4 °C, revealing the presence of some event of the inorganic material, which will be discussed later.

From TG/DTG (Fig. 2c) and DTA (Fig. 2d) curves in N_2, the three initial mass losses and peaks have, respectively, the same assignments that those of the curves in air; however, peaks due to burn of carbonaceous material were not observed. A slow pyrolysis of such residual matter can be seen in the TG curve.

From DSC curves of the dipyrone sodium monohydrate (Fig. 3), it can be observed a broad endothermic peak at 122.9 °C relative to dehydration. This is higher temperature observed in TG curves due to the use of a closed sample holder in the calorimetric experiments. In sequence, one sharp endothermic peak centered at 237.3 °C assigned to the melting ($T_{onset} = 235.4$ °C), followed by an exothermic peak at 244.5 °C due to the first decomposition process of dipyrone sodium monohydrate, was also observed.

The small differences in temperature ranges for these events in TG/DTA and DSC curves were attributed to differences in the heating rates and sample masses used in both techniques.

Hot-stage microscopy was performed in order to better understanding of the thermal events that occurred during heating of dipyrone sodium monohydrate. Results corroborated the events observed in DTA and DSC curves. According to these results (Fig. 4), it can be seen that melting process started at 225.3 °C extending up to 226.3 °C.

A yellowing of the sample just above melting can be clearly observed at 229.2 °C confirming that melting is followed by decomposition in agreement with the DSC data in Fig. 4, in which it was possible to observe an exothermic peak referent to the degradation process.

Evolved gas analysis

The evolution of different species along the experiment can be observed in the 3D spectrum (Fig. 5), in which absorbance changes are presented as a function of time and wavenumber.
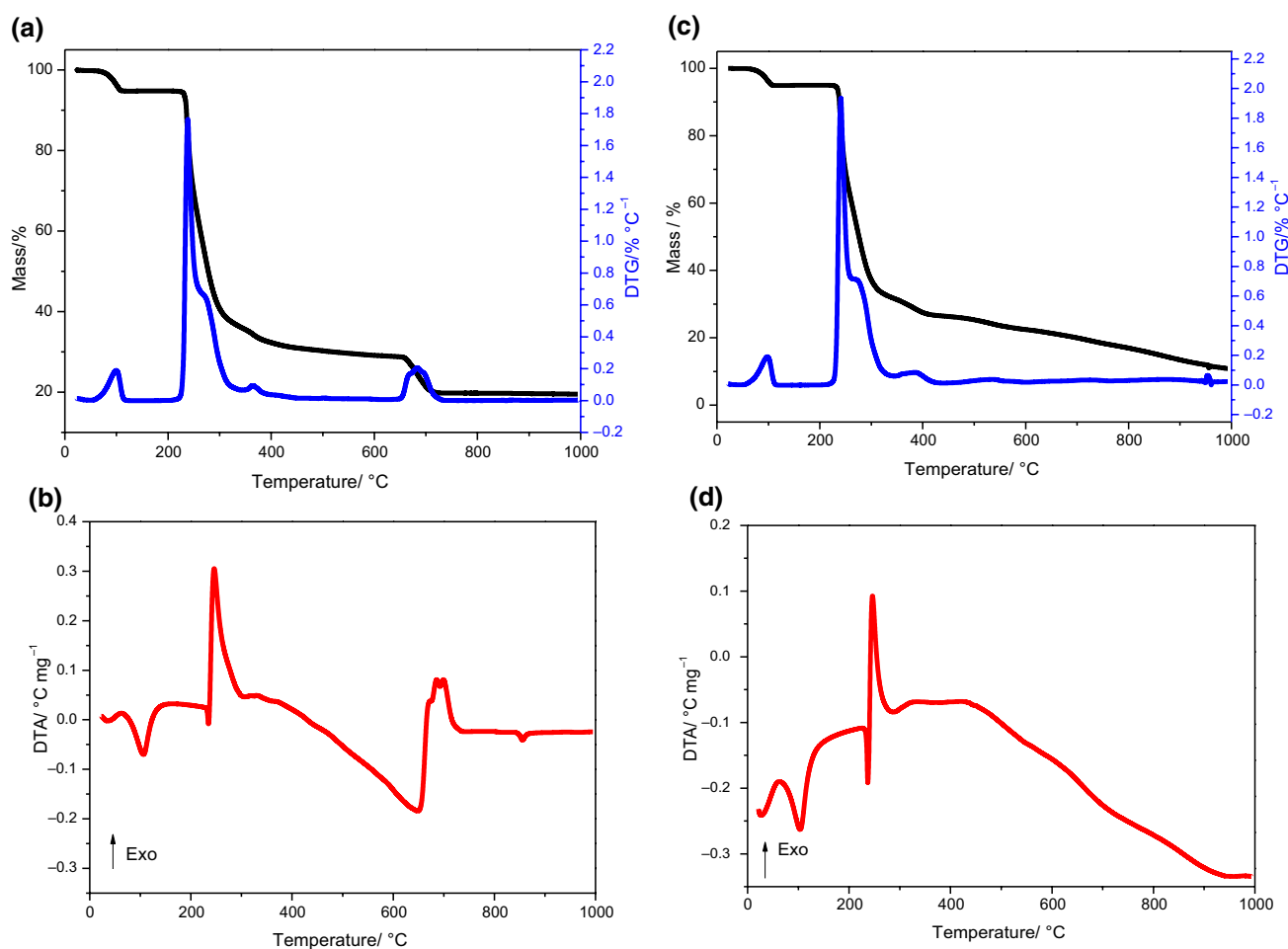
(a)

(b)

(c)

(d)

Fig. 2 TG/DTG and DTA curves of dipyrone sodium monohydrate in dynamic atmosphere of air **a** TG/DTG, **b** DTA and N_2, **c** TG/DTG and **d** DTA; with flow rate of 50 mL min^{-1}, sample mass of 7.0 ± 0.2 mg, in open holder sample of α-alumina, heating rate of 10 °C min^{-1}

In Fig. 6, experimental FTIR spectra at different times of analysis are presented. Along heating of dipyrone sodium monohydrate, signals were observed from 23 min, which corresponds to 252 °C. At 27 min (292 °C), bands at 3081, 3037, 2927, 2266, 2073, 1343, 1169, 1078, 747 and 666 cm^{-1} were observed. At 72 min (742 °C), two bands were observed at 965 and 931 cm^{-1}.

Bands of weak intensity related to sulfur dioxide, benzene, methylamine and isocyanic acid could be observed, when compared to the standards in the library database spectra [17]. The maximum intensity of the bands related to these compounds was reached at 27 min (292 °C), after that bands referent to ammonia were observed with maximum intensity at 78 min (802 °C).

When TG–FTIR results and stoichiometric calculation from TG curve are combined, it can be inferred that decomposition took place with the release of gaseous products in a specific sequence. Firstly, H_2O and SO_2 are released, followed by the concomitant evolution of CH_3NH_2, HNCO,

C_6H_6. After that, signals related to NH_3 were also observed. Moreover, there was release of CO_2.

Data obtained in this work by different techniques suggest the presence of Na_2SO_4 at 500 °C and 1000 °C, corroborating with the depicted by Ribeiro and co-workers [7]. However, the release of gaseous SO_2 occurred in a temperature distinct from that described by Ribeiro et al. (580–740 °C) [7]. According to results of TG–FTIR, it is possible to observe SO_2 release from 252 °C (Fig. 6), which was confirmed by stoichiometric calculations in TG curve.

Characterization of decomposition intermediates

To characterize the intermediates formed during dipyrone thermal decomposition, the sodium monohydrate salt was heated up to 235 °C and the resulting material was collected and submitted to HPLC–MS analysis. The results are presented in Fig. 7.
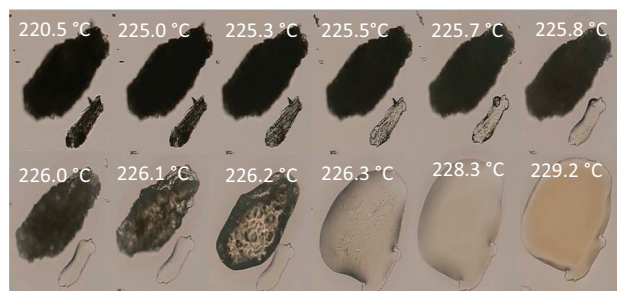
Table 2 Proposition of events, mass loses and temperature ranges, from TG/DTA curves of dipyrone sodium monohydrate in air and N_2 atmospheres

Process	TG data			DTA peaks/°C
	T_{range}/°C	Mass loss/%		
		Exp	Cal	
Air				
$C_{13}H_{16}N_3NaO_4S \cdot H_2O_{(s)} \rightarrow C_{13}H_{16}N_3NaO_4S_{(s)} + H_2O_{(g)}$	53.9–119.1	5.07	5.12	105.1 (endo)
$C_{13}H_{16}N_3NaO_4S_{(s)} \rightarrow C_{13}H_{16}N_3NaO_4S_{(l)}$	–	–	–	235.0 (endo)
$C_{13}H_{16}N_3NaO_4S_{(l)} \rightarrow Na_2SO_{4(s)} + SO_{2(g)} + CH_3NH_{2(g)} + HNCO_{(g)} +$ reaction intermediates	230.8–270.4	39.9	39.4	245.4 (exo)
Reaction intermediates $\rightarrow C_6H_{6(g)} + NH_{3(g)} +$ carbonaceous residue $_{(s)}$	270.4–651.6	26.1	27.1	321.3 (exo); 409.5 (exo);
Burning of carbonaceous $\rightarrow Na_2SO_{4(s)}$	651.6–736.4	8.9	–	701.5 (exo)
$Na_2SO_{4(s)} \rightarrow Na_2SO_{4(l)}$	–	–	–	855.4 (endo)
Residue	1000.0	19.5	20.2	–
Nitrogen				
$C_{13}H_{16}N_3NaO_4S \cdot H_2O_{(s)} \rightarrow C_{13}H_{16}N_3NaO_4S_{(s)} + H_2O_{(g)}$	57.7–117.2	5.10	5.12	103.2 (endo);
$C_{13}H_{16}N_3NaO_4S_{(s)} \rightarrow C_{13}H_{16}N_3NaO_4S_{(l)}$	–	–	–	235.0 (endo);
$C_{13}H_{16}N_3NaO_4S_{(l)} \rightarrow Na_2SO_{4(s)} + SO_{2(g)} + CH_3NH_{2(g)} + HNCO_{(g)} +$ reaction intermediates	229.2–269.1	40.4	39.4	246.4 (exo);
Reaction intermediates $\rightarrow C_6H_{6(g)} + NH_{3(g)} +$ carbonaceous residue $_{(s)}$	269.1–436.9	27.9	27.1	321.3 (exo); 406.6 (exo);
Slow pyrolysis of carbonaceous residue $\rightarrow Na_2SO_{4(s)} + Na_{(g)}$	436.9–1000.0	15.6	–	–
Residue	1000.0	10.9	–	–
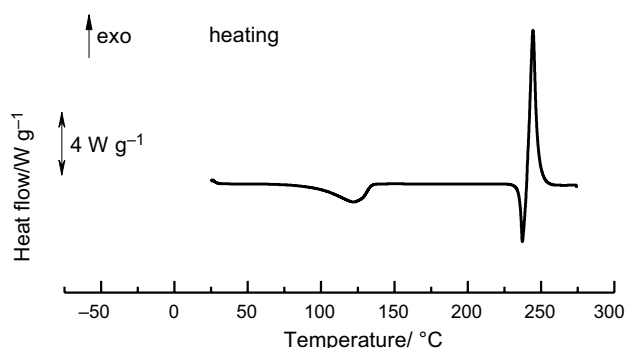
Fig. 3 DSC curves of dipyrone sodium monohydrate in N_2 atmosphere flowing at 50 mL min^{-1}, sample mass of *c.a.* 4.0 mg, in aluminum sample holder with a central pin hole in the lid, heating rate of 10 °C min^{-1}

Fig. 4 Hot-stage micrographs of dipyrone monohydrate sodium in different temperatures, from 220.5 to 229.2 °C, magnification of 200×

The chromatogram presented in Fig. 7a reveals a first significant broad peak at 1.83 min. The fragmentogram referent to the eluate in this retention time (Fig. 7b) suggests the presence of aminopyrine and a second substance whose molecular ion presents a *m/z* ratio of 294.94 g mol^{-1} (M + 1), equivalent to a molecular formula $C_{13}H_{16}N_3O_3S$. Aminopyrine was identified according to the standard fragmentogram [18] in Fig. 7b.

In sequence, a set of peaks between 2.63 and 2.90 min (Fig. 7c) could be found. This result was obtained using chromatographic conditions similar to those suggested by Senyuva et al. [10] described in experimental section and could not be better resolved even after some trials under different experimental conditions for HPLC separation. The fragmentograms contain some of the peaks from aminopyrine and the partial overlapping in the set of peaks suggests the presence of compounds with similar structure. The presence of 4-methylaminopyrine in all of them is evident, as confirmed by the signals in the *m/z* 216.88, 123.04, 118.88 and 82.44 and the standard fragmentogram [19] (Fig. 7c).

The main differences in the three experimental fragmentograms in Fig. 7c can be observed between *m/z* 268 and 276. In this region, while the relative intensities of peak at *m/z* 268 decrease, the *m/z* of triplet at 271–276 increased for
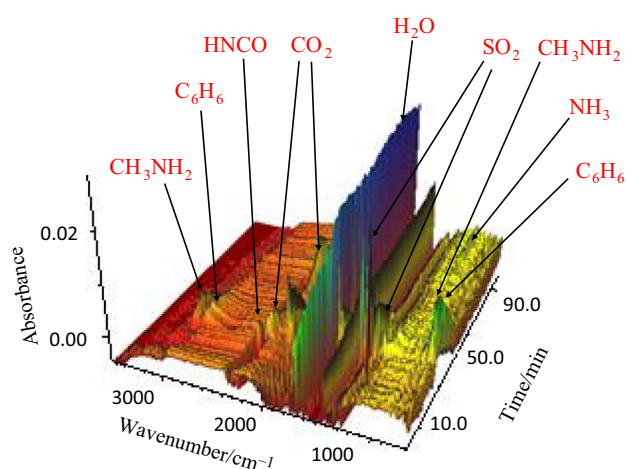
Fig. 5 3D-FTIR spectra of the gaseous products evolved during dipyrone sodium monohydrate heating

higher retention times. This suggests that a structure with molecular formula such as $C_{11}H_{13}N_3O_3S^{\cdot}$ is present at m/z 268 (M + 1) and $C_{13}H_{13}N_3O_2S^{\cdot}$ appeared at m/z 276 (M + 1).

These findings are in partial agreement with the observations of Isaacs et al. [19] who found that aminopyrine and 4-methylaminopyrine are formed when working with GC–MS and dipyrone monohydrated salt was heated in

the GC furnace. However, these authors did not describe the presence of these other structures, probably due to the difference in heating mode of TG and GC techniques. In GC only, the compounds that evaporate are detected, while in TG the degradation occurs step by step and a mixture of reactants and products is collected in the furnace at a pre-established temperature and then injected in the HPLC–MS system.

As a partial conclusion from the HPLC–MS results, it seems that two main groups of decomposition intermediates can be found when dipyrone sodium salt monohydrate is heated just after its melting:

- Those in peak at $t_R = 1.83$ min, one with MM = 294.94 referent to the original molecule, but without hydration water and the Na and one O atoms, and aminopyrine (MM = 230.13), with higher intensity in mass spectra and probably the main product in this group
- Those in the peaks set between t_R 2.63 and 2.90 min in which it is possible to identify a compound with MM = 291.74 (the same as above, but with 3 H atoms less); and other three species with high intensity in mass spectra with MM = 276; 261; 246 and 216, respectively. The last one identified as 4-methylaminopyrine using the standard fragmentogram [19].

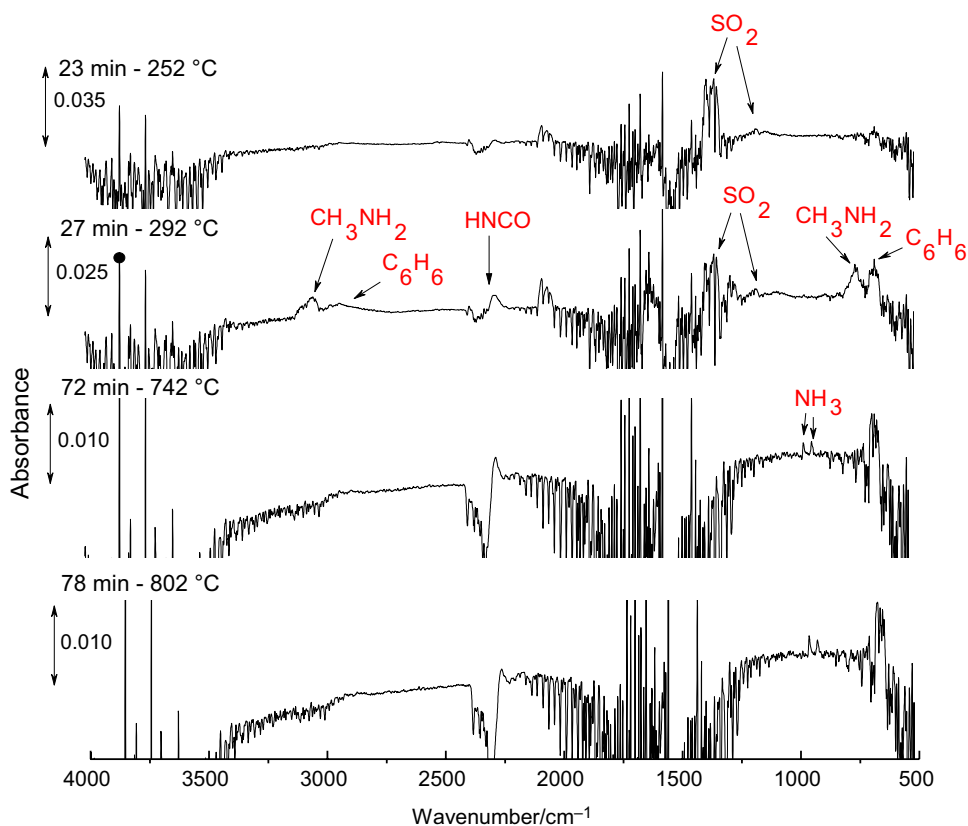**Fig. 6** FTIR spectra of the gases evolved during dipyrone sodium monohydrate heating recorded at different times

Fig. 7 **a** HPLC chromatogram for the residue of dipyrone monohydrate heated up to 235°C. **b** Masses spectra for sample at retention time, 1.83 compared to aminopyrine [18] and **c** Mass spectra for samples at retention times at 2.63, 2.75, 2.90 compared to 4-mehtylaminopyrine [19]
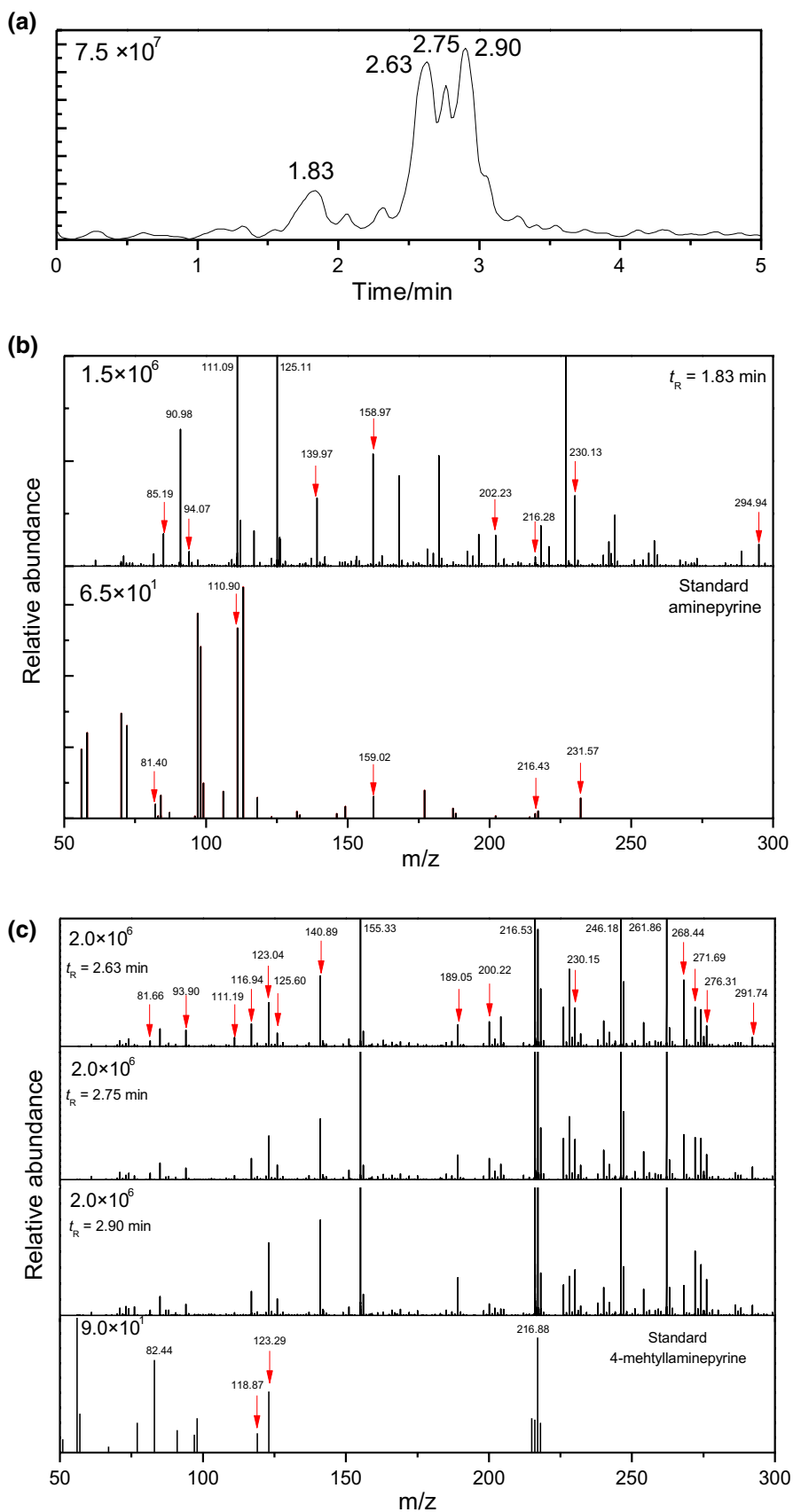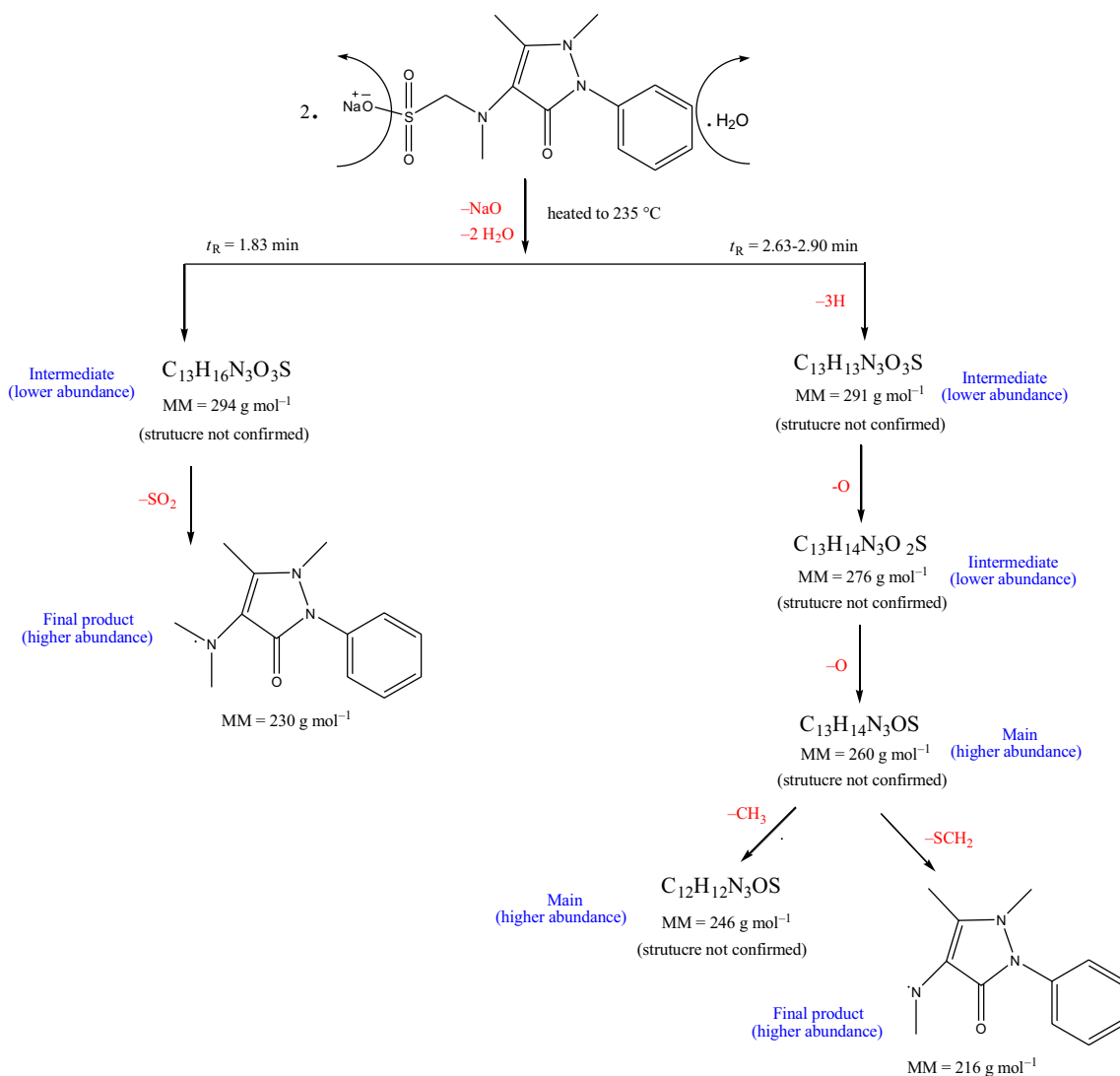
Fig. 8 Products identified in the HPLC–MS experiment for the material collected in the thermobalance after heating the dipyrone sodium monohydrate at 235 °C

In Fig. 8, a representation of the results from HPLC–MS analysis is proposed. In the fragmentograms of peaks at t_R between 2.63 and 2.90 min, the starting structure seems to have 3 H atoms less than the corresponding one at $t_R = 1.83$. Two of these hydrogen atoms could come from the CH_2 bridge between sulfur and nitrogen atoms from sulfonate and tertiary amine groups in the molecule during the loss of the Na and O atoms.

Inorganic residue characterization

As said above, the amount of inorganic residue generated during thermal decomposition of dipyrone sodium monohydrate varies depending on experimental conditions. In addition, while Isaac et al. [9] claim that sodium hydrogen sulfite can be formed by hydrolytic process, Ribeiro et al. [7] described sodium sulfate as the final residue of dipyrone thermal degradation.

In the present work, we observed that the amount of residue varies between experiments, ranging from 19 up to 22% in five experiments under different experimental conditions as summarized in Table 3.

The TG curves related to these residues are presented in Fig. 9, that depicts curves in the 500–1000 °C range, in which carbonaceous residue and the inorganic fraction of the molecule are present. In these curves, it is possible to observe differences in the thermal behavior of inorganic portion in the 550–750 °C range in both TG/DTG (Fig. 9a) and in DTA (Fig. 9b). These differences are probably due to different experimental conditions that affect the thermoanalytical results, as discussed in the classical books as the one from Wendlandt [11].

Table 3 Sample masses, heating rate and residue obtained at 1000 °C, from different TG curves

Atmosphere	Curve in Fig. 9a	Sample mass/mg	Heating rate/°C min^{-1}	Temperature interval/°C	Mass loss/%
Air	1	3.00[a]	10	25–950	78.1
				Residue	21.9
	2	3.00[b]	10	25–950	77.8
				Residue	22.2
	3	7.00[a]	10	25–950	80.5
				Residue	19.5
	4	7.00[a]	25	25–950	80.9
				Residue	19.1
	5	17.00[a]	10	25–950	80.8
				Residue	19.2
N_2	6	7.00[a]	10	25–950	89.1
				Residue	10.9
				Calculated for Na_2SO_4 residue	20.2

[a]Powdered sample

[b]Pressed pellet

]
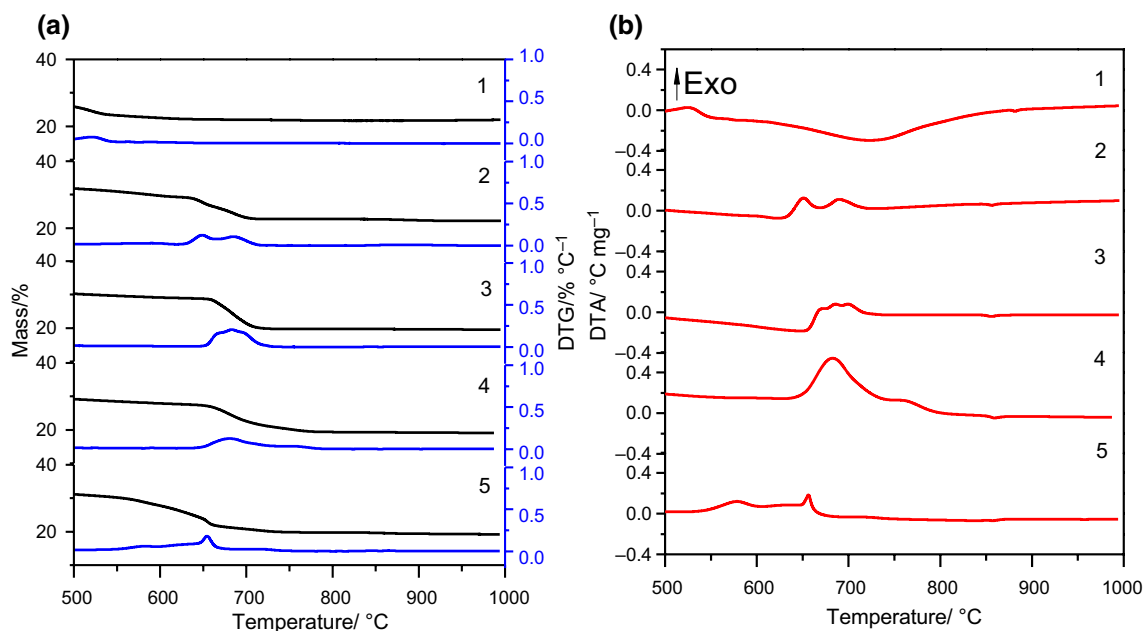
Fig. 9 a TG/DTG and **b** DTA curves obtained from different conditions: (1) 3.00 mg of sample (powder), (2) 3.00 mg of sample (pressed), (3) 7.00 mg of sample (powder), (4) 7.00 mg of sample (powder) and (5) 17.0 mg of sample (powder). All experiments performed in dynamic atmosphere of air, heating ratio 10 °C min^{-1}, except curve 4 that was obtained at 25 °C min^{-1}

The different conditions used in these curves actually revealed that the furnace atmosphere, sample mass, sample presentation in fact affect the amount of residue at the end of the curve at 1000 °C, while heating rate does not seems to play a significant role.

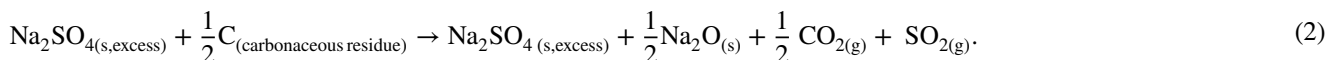These residues were characterized by XRD at 500 and 1000 °C, revealing the presence of sodium sulfate, probably produced in the first degradation step in which SO_2 is liberated, according to the TG–FTIR evolved gas analysis, by a reaction like:

$$2RSO_3^- Na^+ \rightarrow R^1 + R^2 + SO_{2\,(g)} + Na_2SO_{4\,(s)}, \qquad (1)$$
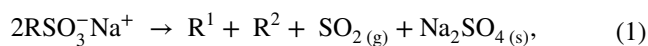
where R^1 and R^2 are residues identified as above.

The different residue amounts presented in Table 3, suggests that the carbonaceous residue varies depending on the

experimental conditions and for higher sample masses, the amount is higher and can reduce part of sodium sulfate to sodium oxide according to Eq. (2):

considering the differences in experimental conditions used in both cases.

The result obtained in N_2 is the lowest residue in the

$$Na_2SO_{4(s,excess)} + \frac{1}{2}C_{(carbonaceous\ residue)} \rightarrow Na_2SO_{4\ (s,excess)} + \frac{1}{2}Na_2O_{(s)} + \frac{1}{2}CO_{2(g)} + SO_{2(g)}. \quad (2)$$

Smaller initial sample masses produce a slighter higher residue, probably due to a higher area of the sample exposed to the oxidative atmosphere, resulting in less carbonaceous material generated during the organic fraction decomposition. Using larger initial masses, higher amounts of carbonaceous matter are generated leading to a partial reduction of the residue as represented by Eq. (2).

As the atmosphere is air, when smaller masses are used, the carbonaceous residue seems to react with the atmosphere gas and not with the sulfate once it is not protected inside the residual material. In larger sample masses, the residual mass seems to protect the residue from the furnace atmosphere, allowing the partial reduction of the sulfate as presented in Table 3. The endothermic signals observed at *c.a.* 850 °C in DTA curves in Fig. 9b are similar to that related to melting of Na_2SO_4 as reported by Jaszczak-Figiel and Gontarz [16],

series, corroborating the proposal of the partial reduction in the presence of carbonaceous residue, formed in higher amount under inner atmosphere. However, the Merck Index [20] describes the decomposition of N_2O at > 400 °C and boiling of metallic sodium at 881.4 °C, leading to suppose that the residue in N_2 is actually Na_2SO_4.

The presence of Na_2SO_4 is also confirmed by FTIR spectra of residue at 500 and 1000 °C, as presented in Fig. 10, obtained in the thermobalance under air, using initial sample mass of 17 mg. Figure 10a presents FTIR spectra of dipyrone sodium monohydrate, the intermediate collected at 500 °C and the sodium sulfate. In this figure, it can be observed that the spectrum of the sample is different from dipyrone itself, but clearly presented bands of sodium sulfate. Additional bands can be observed, related to the presence of carbonaceous matter. The sample collected at 500 °C
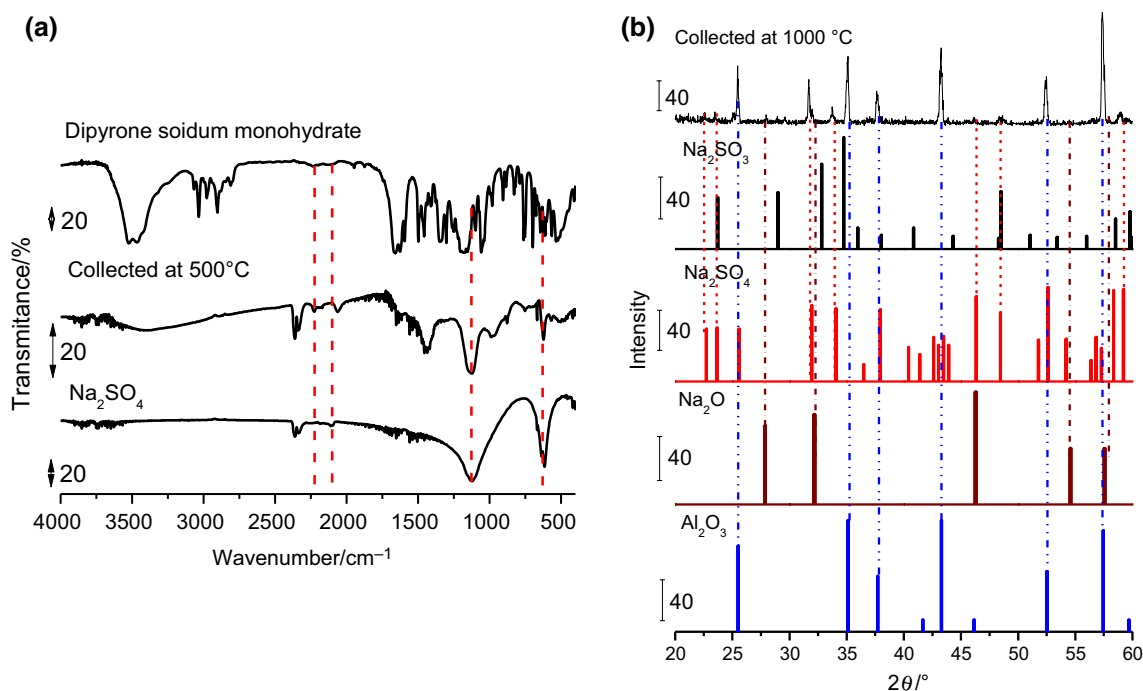

Fig. 10 a FTIR spectra of dipyrone sodium monohydrate, sample collected at 500 °C and Na_2SO_4, **b** comparison of sample collected at 1000 °C, Na_2SO_3, Na_2SO_4, Na_2O and (d) Al_2O_3 from database diffractograms [12–15]
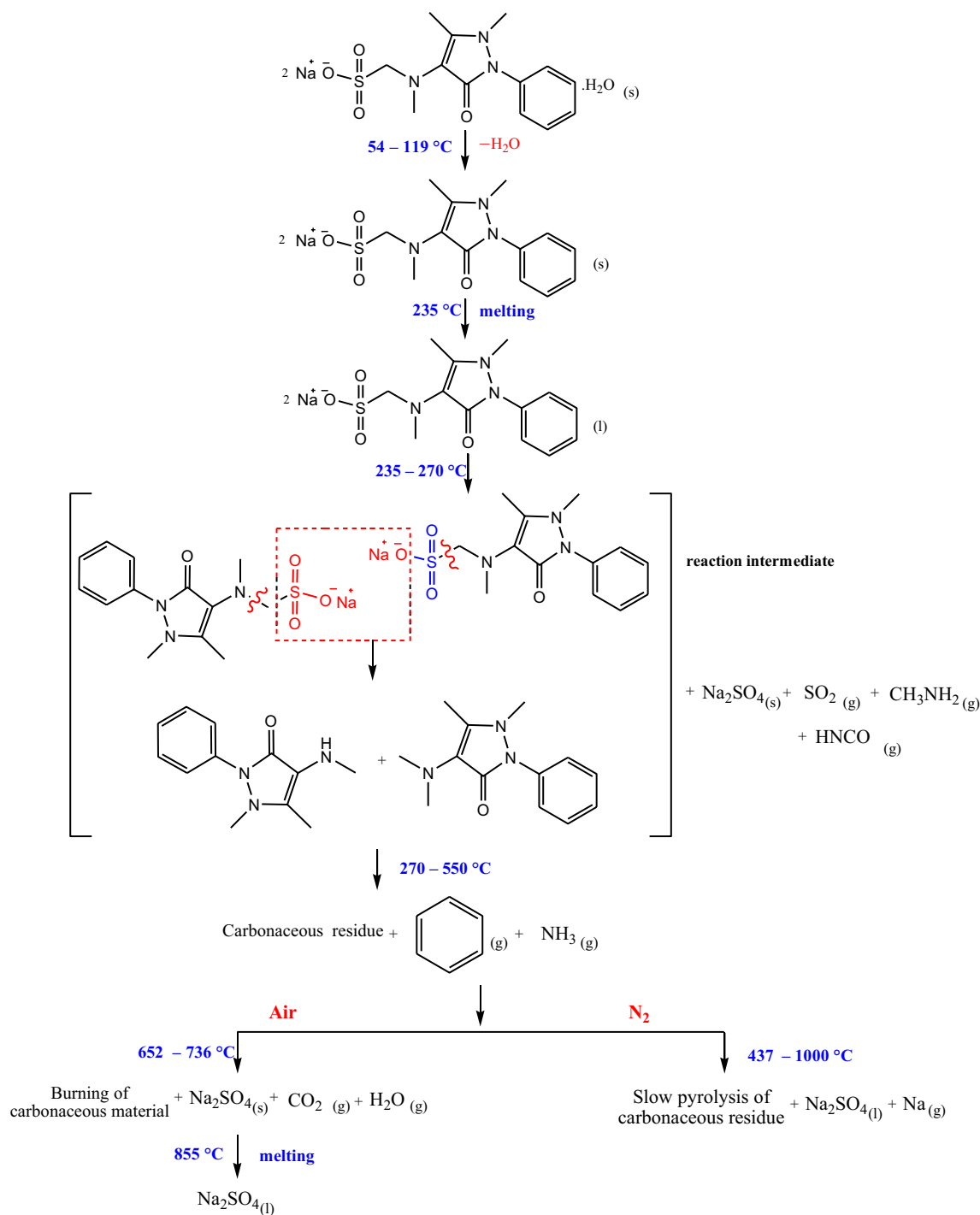
Fig. 11 Proposed thermal behavior for dipyrone sodium monohydrate

suggests that the material presents low crystallinity and its XRD profile is not depicted in Fig. 10.

The residue at 1000 °C presented higher crystallinity degree and it was possible to obtain its XRD patterns; however, the amount of residue was so small that it must be supported in the α-Al$_2$O$_3$ crucible. Figure 10b presents the XRD patterns of the residue at 1000 °C, sodium sulfite,

sodium sulfate, sodium oxide and α-Al$_2$O$_3$, for comparison. It is clear that the most intense peaks are coincident with peaks from α-Al$_2$O$_3$, but at the same time, most of the remaining peaks are coincident with sodium sulfate rather than sulfite.

Thus, one can conclude that sodium sulfate is the main residue formed in the beginning of the decomposition

process when the dipyrone sodium monohydrate molecule loses SO_2. Some sodium oxide can also be formed in the presence of carbonaceous matter produced during the degradation process of dipyrone sodium monohydrate, depending on the experimental conditions.

Proposal of a thermal degradation mechanism for dipyrone sodium monohydrate

Based on all the results discussed above, one can propose a tentative mechanism for the thermal degradation of sodium dipyrone monohydrate. It seems that after dehydration and melting, two molecules are involved in the formation of the Na_2SO_4 with simultaneous release of gaseous SO_2. In such process, one molecule gives Na, S and 3O and the other one gives Na and the last O. For such reaction, it is necessary the break of a S–C bond in one molecule and fragilization of the S–C–N in the other. This explains the presence of aminopyrine and 4-aminopyrine, respectively. A representation of this idea is presented in Fig. 11.

The HPLC–MS results corroborate this proposition, once two groups of molecules could be identified, some intermediates are formed during the thermal degradation process as described in Fig. 8, but aminopyrine and 4-methylaminopyrine are the final intermediate products. Sodium sulfate formed in the first decomposition step end remains as main final inorganic residue at 1000 °C.

Conclusions

Thermal behavior of dipyrone sodium monohydrate was studied by TG/DTG/DTA, DSC, hot-stage microscopy, TG–FTIR, XRD and HPLC–MS. The curves revealed the dehydration and decomposition process in a similar way in dry air and in nitrogen atmospheres. DSC curve presented two endothermic peaks related to dehydration and dipyrone melting, followed by an exothermic peak related to thermal decomposition. Stoichiometric calculations combined with TG–FTIR and HPLC–MS revealed that dipyrone sodium monohydrate decomposes with the evaluation of water, sulfur dioxide, methylamine, isocyanic acid, benzene and ammonia. XRD and FTIR confirmed that inorganic residue collected at 500 °C was Na_2SO_4 as well as when the residue is collected at 1000 °C. However, depending on the condition of the experiments, it can be observed a mixture of Na_2SO_4 and Na_2O or only sodium sulfate. These data have not been described in the literature, besides allow to clarify the doubt about residue end. These results represent the main contribution of the present work, in which the thermal behavior to drug is discribed in detail.

Author contributions RSM contributed to conceptualization, data curation, formal analysis, investigation, methodology, validation, visualization, roles/writing—original draft and writing—review and editing. APGF contributed to conceptualization, data curation, formal analysis, investigation and writing—review and editing. ETGC contributed to conceptualization, data curation, formal analysis, funding acquisition, investigation, methodology, project administration, resources, supervision and writing—review and editing.

References

1. Nikolova I, Tencheva J, Voinikov J, Petkova V, Benbasat N, Danchev N. Metamizole: a review profile of a well-known "forgotten" drug. Part I: pharmaceutical and nonclinical profile. Biotechnol Biotechnol Equip. 2012;26:3329–37. https://doi.org/10.5504/BBEQ.2012.0089.
2. Maione S, Radanova L, Gregorio D, Luongo L, Petrocellis L, Marzo V, Imming P. Effects of metabolites of the analgesic agent dipyrone (metamizol) on rostral ventromedial medulla cell activity in mice. Eur J Pharmacol. 2015;748:115–22. https://doi.org/10.1016/j.ejphar.2014.12.022.
3. Rogosch T, Sinning C, Podlewski A, Watzer B, Schlosburg J, Lichtman AH, Cascio MG, Bisogno T, Di Marzo V, Nüsing R, Imming P. Novel bioactive metabolites of dipyrone (metamizole). Bioorg Med Chem. 2012;20:101–7. https://doi.org/10.1016/j.bmc.2011.11.028.
4. Giron D. Thermal-analysis and calorimetric methods in the characterization of polymorphs and solvates. Thermochim Acta. 1995;248:1–59. https://doi.org/10.1016/0040-6031(94)01953-E.
5. Giordano F, Novak C, Moyano JR. Thermal analysis of cyclodextrins and their inclusion compounds. Thermochim Acta. 2001;380:123–51. https://doi.org/10.1016/S0040-6031(01)00665-7.
6. Valladão DMS, Oliveira LCS, Zuanon Netto J, Ionashiro M. Thermal decomposition of some diuretic agents. J Therm Anal. 1996;46:1291–9. https://doi.org/10.1007/BF01979243.
7. Ribeiro YA, Oliveira JDS, Leles MIG, Juiz AS, Ionashiro M. Thermal decomposition of some analgesic agents. J Therm Anal. 1996;46:1645–55. https://doi.org/10.1007/BF01980770.
8. Schnitzler E, Lençone K, Kobelnik M. Characterization of pharmaceuticals by thermal analysis. Ciências Exatas e da Terra, C Agrárias e Engenharias. 2002;8:91–100.
9. Isaacs RCA, Harper MM, Miller EC. Analytical challenges in the confirmative identification of dipyrone as an adulterant in illicit drug samples. Forensic Sci Int. 2017;270:185–92.
10. Senyuva HZ, Aksahin I, Ozcan S, Kabasakal BV. Rapid, simple and accurate liquid chromatography-diode array detection validated method for the determination of dipyrone in solid and liquid dosage forms. Anal Chim Acta. 2005;547:73–7. https://doi.org/10.1016/j.aca.2004.12.053.
11. Wendlandt WW. Thermal analysis. Wiley; 1986.
12. Fischmeister H. Die Raumgruppe von Na_2CrO_4. Acta Crystallogr. 1954;7:776.
13. Swanson H. Standard X-ray diffraction powder patterns. Fuyat Natl Bur Stand (US) Circ. 1954;539:3–60.
14. Dana's system of mineralogy, 7th ed. New Kensington: Aluminum Co. of America.

15. Zintl E, Baumbach HH. Über Natriumoxyd. Z Anorg Chem. 1931;198:92.
16. Jaszczak-Figiel B, Gontarz Z. Stages of thermal decomposition of sodium oxo-salts of sulphur. J Therm Anal Calorim. 2009;1(96):147–54. https://doi.org/10.1007/s10973-008-9195-8.
17. Nicolet-ThermoScientific Co. Nicolet EPA Vapor Phase data-base. Omnic 8.0 software. Madison: ThermoScientific.
18. https://metabolomicsusi.ucsd.edu/spectrum/?usi=mzspec:MASSBANK:EA070210; accessed: 20 April 2020;
19. https://massbank.eu/MassBank/RecordDisplay.jsp?id=JP003243; Accessed 20 Apr 2020.